Journal of Applied Mechanics and Technical Physics, Vol. 44, No. 2, pp. 193–197, 2003

WAVE RESISTANCE OF AMPHIBIAN AIRCUSHION VEHICLES DURING MOTION ON ICE FIELDS

V. M. Kozin and A. V. Pogorelova

UDC 624.124:532.595

The steady motion of amphibian aircushion vehicles over water covered with continuous ice is studied. The ice sheet is simulated by a viscoelastic ice plate. An analysis is made of the effect of the aspect ratio of the vehicle, the depth of the water reservoir, and ice characteristics on the wave resistance of the vehicle and the speed of the vehicle at which the wave resistance is maximal.

Key words: *incompressible fluid, ice cover, wave resistance, plate, aircushion vehicle.*

1. The hydrodynamic problem of an amphibian aircushion vehicle (ACV) moving over an ice field is simulated by a system of surface pressures [1] moving on a floating viscoelastic ice plate [2].

Let us consider an infinite region covered with continuous ice, over which a specified system of surface pressures q is moving with velocity u. The coordinate system aligned with the vehicle is located as follows: the xOy plane coincides with the unperturbed ice–water interface, the x axis is directed along the motion of the vehicle, and the z axis is directed vertically upward. It is assumed that water is an ideal incompressible fluid of density ρ_2 and the fluid motion is potential. The ice field is simulated by an initially unstressed, viscoelastic, homogeneous, isotropic plate. The period of wave processes in the ice plate is assumed to be shorter than the ice relaxation time. According to [2], the Kelvin–Voigt law of deformation of a delayed-elastic linear medium [3] is used for ice.

From the above assumptions, the linearized boundary conditions for the fluid velocity potential function $\Phi(x, y, z)$ satisfying the Laplace equation $\Delta\Phi = 0$ are written as

$$\frac{Gh^3}{3}\Big(1 - u\tau_\varphi \frac{\partial}{\partial x}\Big)\nabla^4 w + \rho_1 h u^2 \frac{\partial^2 w}{\partial x^2} + \rho_2 g w - \rho_2 u \frac{\partial \Phi}{\partial x} = -q \qquad \text{for} \quad z = 0,$$

$$\frac{\partial \Phi}{\partial z} = 0 \qquad \text{for} \quad z = -H, \tag{1.1}$$

where $G = 0.5E/(1 + \nu)$ is the shear elastic modulus of ice, E is the elastic modulus of ice under tension and compression, ν is Poisson's coefficient, $h(x, y)$ is the ice thickness, $\rho_1(x, y)$ is the ice density, τ_φ is the strain relaxation time for ice or the "delay" [2, 3], $w(x, y)$ is the displacement of the fluid surface or the vertical displacement of ice, and $H = H_1 - b$, where H_1 is the depth of the basin and $b = \rho_1 h/\rho_2$ is the depth of submergence of ice in static equilibrium. For great depths, where H_1 far exceeds h, one can assume that $H \approx H_1$. Below, we assume that ρ_1 and h are constants. The reduced values of the shear modulus G and the ice density ρ_1 found by integration over the plate thickness [2] should be taken as the calculated values.

According to [1, 4], the wave resistance acting on an ACV is calculated by the formula

$$R = \iint\limits_{\Omega} q \frac{\partial w}{\partial x}\, dx\, dy, \tag{1.2}$$

where Ω is the region of load distribution $q(x, y)$.

Institute of Machine Science and Metallurgy, Far East Division, Russian Academy of Sciences, Komsomol'sk-on-Amur 681005. Translated from Prikladnaya Mekhanika i Tekhnicheskaya Fizika, Vol. 44, No. 2, pp. 49–55, March–April, 2003. Original article submitted November 22, 2001; revision submitted July 9, 2002.

0021-8944/03/4402-0193 $25.00

The linearized kinematic condition at the ice–boundary interface has the form [1]

$$\frac{\partial\Phi}{\partial z}\Big|_{z=0} = -u\,\frac{\partial w}{\partial x}. \tag{1.3}$$

2. We assume that the functions $\Phi(x,y,z)$, $w(x,y)$, and $q(x,y)$ satisfy the conditions necessary for their representation in the form of Fourier integrals in the two variables x and y. Following [4–6], we write

$$\Phi(x,y,z) = \frac{1}{4\pi^2}\int\limits_0^\infty k\,dk\int\limits_{-\pi}^{\pi} d\theta \iint\limits_\Omega (F_1\exp(-kz) + E_1\exp(kz))$$

$$\times\exp(ik((x-x_1)\cos\theta + (y-y_1)\sin\theta))\,dx_1\,dy_1,$$

$$q(x,y) = \frac{1}{4\pi^2}\int\limits_0^\infty k\,dk\int\limits_{-\pi}^{\pi} d\theta \iint\limits_\Omega q(x_1,y_1)\exp(ik((x-x_1)\cos\theta + (y-y_1)\sin\theta))\,dx_1\,dy_1, \tag{2.1}$$

$$w(x,y) = \frac{1}{4\pi^2}\int\limits_0^\infty k\,dk\int\limits_{-\pi}^{\pi} d\theta \iint\limits_\Omega w(x_1,y_1)\exp(ik((x-x_1)\cos\theta + (y-y_1)\sin\theta))\,dx_1\,dy_1,$$

where F_1 and E_1 are the desired functions of the variables x_1, y_1, k, and θ.

Substitution of relation (2.1) into boundary conditions (1.1) using the kinematic condition (1.3) and dependence (1.2), replacement of the variables $k = \lambda$ and $k\cos\theta = \alpha$, and simple transformations yield the following formula for the wave resistance R of the system of surface pressures $q(x,y)$ for steady motion over the ice plate:

$$R = \frac{1}{\pi^2\rho_2 u^2}\int\limits_0^\infty \lambda^2\tanh(\lambda H)\,d\lambda\int\limits_0^\lambda \frac{(C_1^2+C_2^2+C_3^2+C_4^2)\alpha\eta_1\,d\alpha}{\sqrt{\lambda^2-\alpha^2}(\xi_1^2+\eta_1^2)}, \tag{2.2}$$

where

$$C_1 = \iint\limits_\Omega q(x,y)\cos(\alpha x)\cos(y\sqrt{\lambda^2-\alpha^2})\,dx\,dy, \quad C_2 = \iint\limits_\Omega q(x,y)\cos(\alpha x)\sin(y\sqrt{\lambda^2-\alpha^2})\,dx\,dy,$$

$$C_3 = \iint\limits_\Omega q(x,y)\sin(\alpha x)\cos(y\sqrt{\lambda^2-\alpha^2})\,dx\,dy, \quad C_4 = \iint\limits_\Omega q(x,y)\sin(\alpha x)\sin(y\sqrt{\lambda^2-\alpha^2})\,dx\,dy,$$

$$\xi_1 = \alpha^2\Big(1+\frac{\rho_1 h\lambda\tanh(\lambda H)}{\rho_2}\Big) - \frac{Gh^3\lambda^5\tanh(\lambda H)}{3\rho_2 u} - \frac{g\lambda\tanh(\lambda H)}{u^2}, \qquad \eta_1 = \frac{\alpha\tau_\varphi Gh^3\lambda^5\tanh(\lambda H)}{3\rho_2 u}.$$

By analogy with [6, 7], we consider a system of moving pressures $q(x,y)$ described by the function of hyperbolic tangent:

$$q(x,y) = (q_0/4)[\tanh(\alpha_1(x+L/2)) - \tanh(\alpha_1(x-L/2))]$$

$$\times[\tanh(\alpha_2(y+L/(2\omega))) - \tanh(\alpha_2(y-L/(2\omega)))], \tag{2.3}$$

where q_0 is the nominal pressure, L is the vehicle length, $\omega = L/B$ is the aspect ratio of the vehicle, B is the vehicle width, and α_1 and α_2 are the parameters characterizing the degree of deviation of the pressure distributions in the longitudinal and transverse directions from a rectangular form, respectively. The larger the values of α_1 and α_2, the closer the pressure distribution to a rectangle form. As $\alpha_1, \alpha_2 \to \infty$, the pressure $q(x,y)$ tends to the pressure q_0 uniformly distributed over the rectangle. Similarly to [6, 7], we use $\alpha_1 L = \alpha_2 L = 10$ in numerical calculations.

For the steady motion of the pressure system (2.3) over an ice viscoelastic plate, the dimensionless wave-resistance coefficient A is calculated from the formula

$$R/D = Aq_0/(\rho_2 gL), \tag{2.4}$$

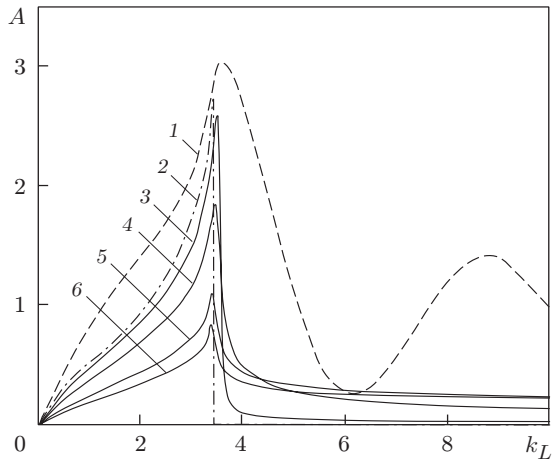

Fig. 1

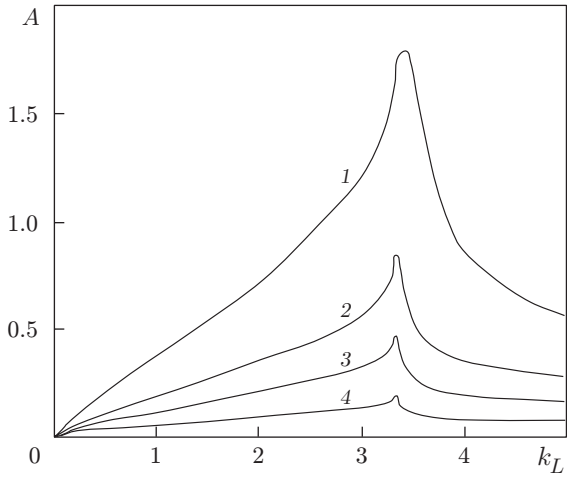

Fig. 2

where

$$A = \frac{\pi^2 \omega k_L}{(\alpha_1 L)^2 (\alpha_2 L)^2} \int\limits_0^\infty \lambda^2 \tanh\,(\lambda\gamma)\, d\lambda \int\limits_0^\lambda \frac{\sin^2(\alpha/2) \sin^2\left(\sqrt{\lambda^2-\alpha^2}/(2\omega)\right) \alpha\eta\, d\alpha}{\sinh^2(\pi\alpha/(2\alpha_1 L)) \sinh^2\left(\pi\sqrt{\lambda^2-\alpha^2}/(2\alpha_2 L)\right) \sqrt{\lambda^2-\alpha^2}\,(\xi^2+\eta^2)},$$

$$D = q_0 LB, \quad k_L = gL/u^2, \quad \omega = L/B, \quad \gamma = H/L,$$

$$\xi = \alpha^2(1 + \varepsilon\chi\lambda \tanh\,(\lambda\gamma)) - æ\chi^3 k_L \lambda^5 \tanh\,(\lambda\gamma) - k_L \lambda \tanh\,(\lambda\gamma),$$

$$\eta = \alpha\tau_0 \sqrt{k_L}\, \chi^3 æ \lambda^5 \tanh\,(\lambda\gamma), \quad \varepsilon = \rho_1/\rho_2, \quad \chi = h/L, \quad \tau_0 = \tau_\varphi \sqrt{g/L}, \quad æ = G/(3L\rho_2 g).$$

Here unlike in relation (2.2), the integration variables are in dimensionless form.

3. Numerical calculations by formula (2.4) were compared with previous theoretical results on the wave resistance for the motion of a vehicle on pure water [7], broken ice [5, 6], and an ideal elastic plate [8]. In addition, a comparison was performed of theoretical and experimental data on the deformation of an ice field during motion of a body over an ice plate [9–13]. The results of the comparison are shown in Figs. 1–6.

The dashed curve 1 in Fig. 1 shows the results of [6, 7] obtained for the steady motion of an ACV on water for $\omega = 2$ and $\gamma = 0.3$. The dash-and-dot curve 2 is obtained for the motion of a load distributed under law (2.3) over an ideal elastic plate for $\omega = 2$, $\gamma = 0.3$, $\varepsilon = 0.9$, $\chi = 0.01$, and $E/(12(1-\nu^2)L\rho_2 g) = 2386$, where $E = 5 \cdot 10^9$ Pa, $\nu = 1/3$, $L = 20$ m, and $\rho_2 = 1000$ kg/m^3. The integral formula for calculating curve 1 is omitted because similar results were obtained in [8], and this curve is given here for comparison. The solid curves (3–6) correspond to calculations by formula (2.4) for dimensionless relaxation times $\tau_0 = 0.07$, 0.7, 3.5, and 7.0 for $\omega = 2$, $\gamma = 0.3$, $\varepsilon = 0.9$, $\chi = 0.01$, and $æ = 3401.4$. An analysis of the behavior of curve 2 shows that the model of an ideal elastic ice in the subcritical velocity region corresponds to zero wave resistance. This conclusion does not agree with the known experimental data [12]. Curve 3 obtained for the model of viscoelastic ice for a short relaxation time $\tau_0 = 0.07$ is close to curve 2, but in the region of small velocities, this model yields nonzero wave resistances. With increase in τ_0, the maximum value of the coefficient A becomes smaller, which is supported by the results of [10, 11]. Studies of the motion of a plane pressure front on viscoelastic ice [10, 11] show that an increase in viscosity leads to a decrease in the maximum amplitude of the vertical displacement of ice. Kozin [12] established that the Kelvin–Voigt model gives the best fit to experimental data for strain relaxation times $\tau_\varphi = 5$–10 sec (for $L = 20$ m and $\tau_0 = 3.5$–7.0). At the same time, using experimental data, Takizava [13] suggested that the relaxation time ranges from 0.2 to 0.8 sec.

Figure 2 shows curves of the wave-resistance coefficient A versus the parameter k_L for various ice depths. Curves 1–4 are plotted for $\chi = 0.005$, 0.010, 0.015, and 0.025, respectively, and $\omega = 2$, $\gamma = 0.3$, $\varepsilon = 0.9$, $æ = 3401.4$, and $\tau_0 = 7$. It can be seen that with increase in ice thickness, the wave resistance decreases. For $\chi = 0.025$ (which corresponds to an ice thickness $h = 0.5$ m and a vehicle length $L = 20$ m), the curve of the wave resistance versus the parameter k_L does not show a "hump" typical of an ACV.

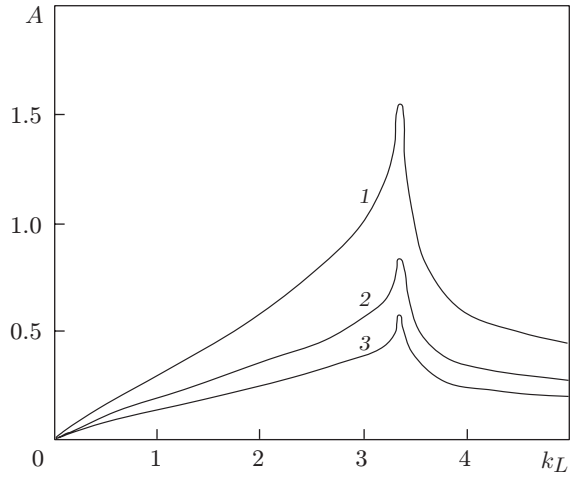

Fig. 3

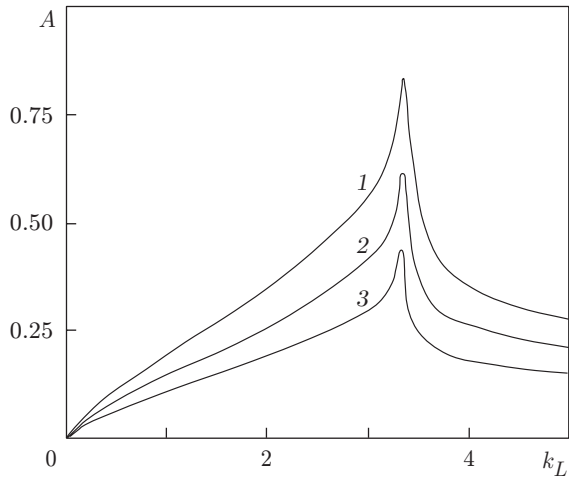

Fig. 4

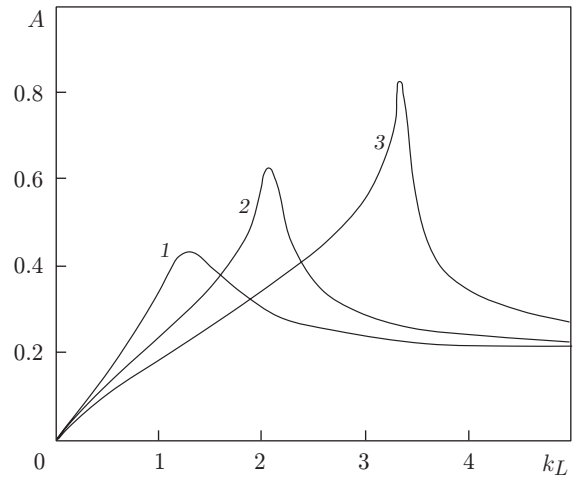

Fig. 5

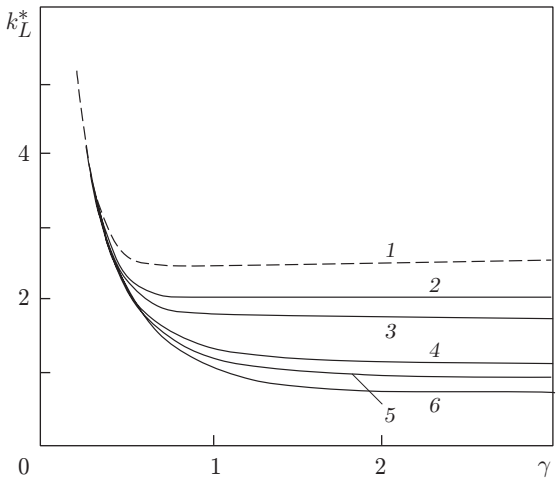

Fig. 6

Figure 3 shows the wave-resistance coefficient A versus the parameter k_L for various aspect ratios of ACVs for $\chi = 0.01$, $\gamma = 0.3$, $\varepsilon = 0.9$, $æ = 3401.4$, and $\tau_0 = 7$. Curves 1–3 correspond to $\omega = 1$, 2, and 3, respectively. As the aspect ratio of the vehicle increases, the wave-resistance coefficient decreases, as in the case of pure water and broken ice [5–7], which is supported by theoretical studies of the deformation of an ideal elastic ice surface under the motion of a rectangular load over this surface [9].

Figure 4 shows curves of the wave-resistance coefficient A versus the parameter k_L for various values of the parameter $æ$, which depends on the ratio of the shear elastic modulus of ice G to the vehicle length L. Curves 1–3 correspond to $æ = 3401.4$, 6802.8, and 13,605.6 for $\omega = 2$, $\chi = 0.01$, $\gamma = 0.3$, $\varepsilon = 0.9$, and $\tau_0 = 7$. From Fig. 4 it follows that if the vehicle length L and the dimensionless parameters ω, χ, γ, ε, and τ_0 are constant, an increase in the elastic modulus of ice leads to a decrease in the wave resistance of ice.

Figure 5 shows curves of the wave-resistance coefficient of the ACV versus the parameter k_L for various relative depths of the water basin. Curves 1–3 are plotted for $\gamma = 1.0$, 0.5, and 0.3 and $\omega = 2$, $\chi = 0.01$, $\varepsilon = 0.9$, $\tau_0 = 7$, and $æ = 3401.4$. An increase in the relative depth of the basin leads to a decrease in the absolute maximum of the wave resistance and the displacement of the maximum point to the high-velocity region.

Figure 6 shows curves of the parameter k_L^* for the maximum wave resistance versus the relative depth γ. The dashed curve 1 is plotted for calculations by formula (2.8) in [6] for the steady motion of an ACV on pure water for $\omega = 2$. The solid curves 2–6 are plotted by formula (2.4) of the present paper with $\varepsilon = 0.9$ and $\omega = 2$. The same curves describe the dependence $k_L^*(\gamma)$ for $\omega = 1$–3. Curves 2 and 3 refer to $\tau_0 = 3.5$ and 7, respectively,

for $\chi = 0.005$ and $æ = 3401.4$, curves 4 and 5 refer to $æ = 3401.4$ and 13,605.6, respectively, for $\chi = 0.01$ and $\tau_0 = 7$, and curve 6 refers to $\tau_0 = 7$, $\chi = 0.025$, and $æ = 3401.4$. In addition, curve 5 refers to the parameters $æ = 3401.4$, $\chi = 0.015$, and $\tau_0 = 7$. An analysis of the behavior of the curves shows that for small relative depths of the water basin ($\gamma \leqslant 0.4$), the effect of the parameters ω, χ, τ_0, and $æ$ on the maximum wave resistance point k_L^* is insignificant. For great depths ($\gamma > 0.4$), an increase in the parameters χ, τ_0, and $æ$ leads to displacement of the point k_L^* to the high-velocity region; the greater the basin depth, the stronger the effect of the parameters χ, τ_0, and $æ$. The conclusion on the effect of the parameters $\chi = h/L$ and $æ = G/(3L\rho_2 g)$ on the critical velocity (corresponding to the maximum wave resistance) is supported by the results of [11]. The studies of [10, 11] show that a variation in viscosity leads to an insignificant displacement of the point of maximum amplitude $w(x, y)$ to the low-velocity region. This conclusion disagrees with the results of our experiments, which is obviously explained by the fact that ice was simulated by different models of viscoelastic bodies. In [10, 11], Maxwell's model is used, whereas we consider the Kelvin–Voigt model [3]. In addition, if we convert from the dimensionless variable k_L^* to the vehicle speed u, the quantity u^*, which corresponds to the maximum wave resistance, obeys the law $u^* = \sqrt{gH}$ for small reservoir depths ($\gamma \leqslant 0.4$). For great depths ($\gamma > 0.4$), the value of u^* lies within the range of $(u_{\min}, \hat{u})$, where $\hat{u} = \sqrt{gH}$, $u_{\min} = 2(Dg^3/(27\rho_2))^{1/8}$ [2], and $D = Eh^3/(12(1-\nu^2))$. For small relaxation times $\tau\varphi$, the quantity u^* is close to $u_{\min}$. This result also agrees with the conclusions of [11, Chapter 7]. In the range $\omega = 1$–3, the aspect ratio of the vehicle has no effect on the value of k_L^*.

In the theoretical studies described above, we established the dependence of the wave resistance of ACVs during motion over ice fields versus the main characteristics of the vehicles and the ice situation. Compared with the results of [8], the solution proposed in the present paper more completely describes the physical processes underlying the occurrence of the wave resistance of ACVs during steady-state motion over ice fields.

The results obtained can be used to estimate the ice-breaking properties of various ACVs for breaking ice by a resonance method [12].

REFERENCES

1. Yu. Yu. Benua, V. K. D'yachenko, B. A. Kolyzaev, et al., *Fundamentals of the Theory of Aircushion Vehicles* [in Russian], Sudostroenie, Leningrad (1970).
2. D. E. Kheisin, *Ice-Field Dynamics* [in Russian], Gidrometeoizdat, Leningrad (1967).
3. A. M. Freudenthal and H. Geiringer, *The Mathematical Theories of The Inelastic Continuum* [Russian translation], Fizmatgiz, Moscow (1962).
4. V. P. Bol'shakov, "Wave resistance of a system of surface pressures," in: *13th Scientific and Technical Conference of Scientific and Technical Society of Shipbuilding Industry on Ship Theory* (Leningrad, September 10–15, 1963), No. 49, Izd. Inst. Krylova, Leningrad (1963), pp. 68–88.
5. V. M. Kozin and A. V. Milovanova, "The wave resistance of amphibian aircushion vehicles in broken ice," *J. Appl. Mech. Tech. Phys.*, **37**, No. 5, 634–637 (1996).
6. V. M. Kozin and A. V. Pogorelova, "Effect of broken ice on the wave resistance of an aircushion vehicle in nonstationary motion," *J. Appl. Mech. Tech. Phys.*, **40**, No. 6, 1036–1041 (1999).
7. L. J. Doctors and S. D. Sharma, "The wave resistance of an aircushion vehicle in steady and acceleration motion," *J. Ship Res.*, **16**, No. 4, 248–260 (1972).
8. A. N. Kovalev, "Determination of the wave resistance of aircushion vehicles during motion over ice field," Doct. Dissertation in Tech. Sci., Nizhnii Novgorod (1998).
9. F. Milinazzo, M. Shinbrot, and N. W. Evans, "A mathematical analysis of the steady response of floating ice to the uniform motion of rectangular load," *J. Fluid Mech.*, **287**, 173–197 (1995).
10. R. J. Hosking, A. D. Sneyd, and D. W. Waugh, "Viscoelastic response of floating ice plate to a moving load," *J. Fluid Mech.*, **196**, 409–430 (1988).
11. V. A. Squire, R. J. Hosking, A. D. Kerr, and P. J. Langhorne, *Moving Loads on Ice Plates*, Kluwer Acad. Publ., Dordrecht (1996).
12. V. M. Kozin, "Substantiation of initial data for selecting the main parameters of aircushion vehicles designed for breaking ice by a resonance method," Candidate's Dissertation in Tech. Sci., Gor'kii (1983).
13. T. Takizava, "Deflection of a floating sea ice sheet induced by a moving load," *Cold Regions Sci. Technol.*, **11**, 171–180 (1985).